Science of the Total Environment 605–606 (2017) 58–65

Contents lists available at ScienceDirect

Science of the Total Environment

journal homepage: www.elsevier.com/locate/scitotenv

# Interactions between stepwise-eluted sub-fractions of fulvic acids and protons revealed by fluorescence titration combined with EEM-PARAFAC

Fanhao Song [a], Fengchang Wu [a], Fei Guo [a], Hao Wang [a], Weiying Feng [a], Min Zhou [b], Yanghui Deng [a], Yingchen Bai [a,*], Baoshan Xing [c], John P. Giesy [a,d]

[a] State Key Laboratory of Environmental Criteria and Risk Assessment, Chinese Research Academy of Environmental Science, Beijing 10012, China
[b] School of Environmental and Municipal Engineering, Qingdao University of Technology, Qingdao 266033, China
[c] Stockbridge School of Agriculture, University of Massachusetts, Amherst, MA 01003, USA
[d] Department of Biomedical and Veterinary Biosciences, Toxicology Centre, University of Saskatchewan, Saskatoon, Saskatchewan, SK S7N 5B3, Canada

## HIGHLIGHTS

- Fluorescence titrations of FA sub-fractions with proton were visited by EEM-PARAFAC.
- Carboxylic/phenolic/protein-like chromophores were identified in PARAFAC components.
- $pK_{a1}$ and $pK_{a2}$ of fulvic-like components were 2.43–4.13 and 9.95–11.27, respectively.
- $pK_{a1}$ and $pK_{a2}$ of protein-like components were 3.33–4.22 and 9.77–10.13, respectively.

## GRAPHICAL ABSTRACT

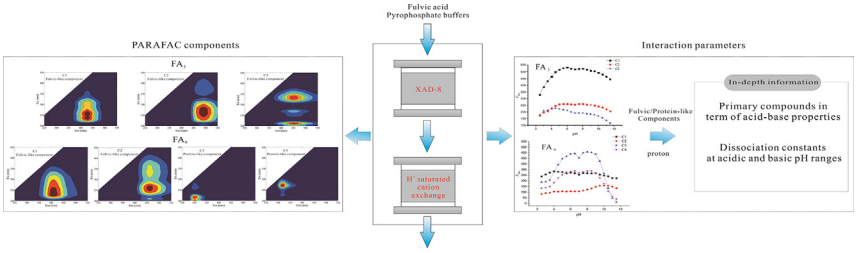


## ARTICLE INFO

*Article history:*
Received 14 April 2017
Received in revised form 16 June 2017
Accepted 20 June 2017
Available online xxxx

Editor: Jay Gan

*Keywords:*
Binding
Functional groups
Fulvic-like components
Protein-like components
Dissociation constant

## ABSTRACT

In aquatic environments, pH can control environmental behaviors of fulvic acid (FA) via regulating hydrolysis of functional groups. Sub-fractions of FA, eluted using pyrophosphate buffers with initial pHs of 3.0 ($FA_3$), 5.0 ($FA_5$), 7.0 ($FA_7$), 9.0 ($FA_9$) and 13.0 ($FA_{13}$), were used to explore interactions between the various, operationally defined, FA fractions and protons, by use of EEM-PARAFAC analysis. Splitting of peaks ($FA_3$ and $FA_{13}$), merging of peaks ($FA_7$), disappearance of peaks ($FA_9$ and $FA_{13}$), and red/blue-shifting of peaks were observed during fluorescence titration. Fulvic-like components were identified from $FA_3$-$FA_{13}$, and protein-like components were observed in fractions $FA_9$ and $FA_{13}$. There primary compounds (carboxylic-like, phenolic-like, and protein-like chromophores) in PARAFAC components were distinguished based on acid-base properties. Dissociation constants ($pK_a$) for fulvic-like components with proton ranged from 2.43 to 4.13 in an acidic pH and from 9.95 to 11.27 at basic pH. These results might be due to protonation of di-carboxylate and phenolic functional groups. At basic pH, $pK_a$ values of protein-like components (9.77–10.13) were similar to those of amino acids. However, at acidic pH, $pK_a$ values of protein-like components, which ranged from 3.33 to 4.22, were 1–2 units greater than those of amino acids. Results presented here, will benefit understanding of environmental behaviors of FA, as well as interactions of FA with environmental contaminants.



## 1. Introduction

Fulvic acid (FA) is a more mobile hydrophobic acid fraction of dissolved organic matter (DOM) ubiquitously existing in water and soil environments (Bai et al., 2015; Lehmann and Kleber, 2015). FA has

* Corresponding author.
*E-mail address:* baiyc@craes.org.cn (Y. Bai).

http://dx.doi.org/10.1016/j.scitotenv.2017.06.164
0048-9697/

potential effects on transport and bioavailability of nutrients, metals, polycyclic aromatic hydrocarbons, and other contaminants (Cabaniss and Shuman, 2002; Cai et al., 2016; Dai et al., 2006; Giesy et al., 1978; Giesy et al., 1983; Leversee et al., 1983; Wang et al., 2016; Xia et al., 2009). In various aquatic systems, factors including pH, temperature, and salinity can affect physical and chemical behaviors of FA (Gao et al., 2015; Pace et al., 2012; Sun et al., 2016; Yu et al., 2010b). Effects of increasing or decreasing pH on molecular structures, functionalities, conformations, and intermolecular interactions of FA with metal ions have been reported (Giesy, 1983; Giesy et al., 2010; Giesy et al., 1986; Midorikawa and Tanoue, 1998; Pace et al., 2012; Timko et al., 2015; Tipping, 2005; Yan et al., 2013). For example, based on fluorescence properties, it can be demonstrated that pH can affect molecular orbitals of excitable electrons and sphero-colloidal configurations of FA (Pace et al., 2012; Yan et al., 2013). The pH can affect molecular sizes of FA by partial disassembling of small groups at lower pHs, and formation of additional inter-/intra-molecular hydrogen bonds at neutral pH (Pace et al., 2012; Piccolo et al., 1999; Romera-Castillo et al., 2014). Dissociation constants of fluorescent ligands of DOM binding with protons are associated with the protonation of carboxylates, which, based on pH-dependence of fluorescence, are candidate ligands (Midorikawa and Tanoue, 1998; Wu and Tanoue, 2001).

Although mechanisms of interactions between FA and proton have been studied, due to the structural heterogeneity and variety of compositions, as well as the challenged operational separation of FA, it is not well understood (Bai et al., 2015; Lehmann and Kleber, 2015). Fractionating FA into sub-fractions can reduce their heterogeneity, which facilitates exploration of origin, structure and evolution, as well as interactions with chemical species. Successful isolation of standard sub-fractions of FA derived from Chinese sources was accomplished by use of stepwise elution from XAD-8 with pyrophosphate buffers. Detailed descriptions of isolation, fractionation and characterization of FA sub-fractions have been reported previously (Bai et al., 2015). Enrichment of protein-like substances was also reported in FA sub-fractions; however the possible chemical characters of protein-like substances have not yet been studied.

Fluorescence excitation-emission matrix (EEM) spectroscopy is a rapid, inexpensive, sensitive, elective and non-destructive technique to investigate chemical and physical properties of DOM. The EEM combined parallel factor analysis (PARAFAC) technique has been used to characterize fluorescence features of DOM in aquatic systems by decomposing three-way data into individual fluorescence components without any assumptions about spectral shape or number (Bro, 1997; Sgroi et al., 2016; Stedmon and Bro, 2008; Zhang et al., 2011). EEM-PARAFAC analyses have been used to explore interactions of individual fluorescence components with metals and organic contaminants (Cory and Mcknight, 2005; He et al., 2013; Kowalczuk et al., 2009; Maqbool and Hur, 2016; Sgroi et al., 2016; Wei et al., 2016; Wu et al., 2011; Yan et al., 2013; Yu et al., 2011; Zhang et al., 2011). Conditional stability constants were also calculated for the interactions between PARAFAC components of DOM and metal ions (e.g., $Cu^{2+}$, $Hg^{2+}$), as well as organic contaminants (e.g., sodium dodecyl sulfate) using EEM-PARAFAC (Maqbool and Hur, 2016; Yamashita and Jaffé, 2008). However, to the best of our knowledge, p$K_a$ values of PARAFAC components of FA at acidic and basic pH ranges had not yet been established.

Objectives of this study were to: (1) Determine primary constituents based on acid-base properties of PARAFAC components; (2) Investigate the possible environ-chemical behaviors of protein-like components with pH changing; (3) Calculate and compare the p$K_a$ values of PARAFAC components at acidic and basic pH ranges.

## 2. Materials and methods

### 2.1. Sample pretreatment and fluorescence titration

The Chinese standard FA sample was isolated from surface soil collected from the Jiufeng Mountain Forest, Beijing, China. Extraction and purification of FA were performed according procedures recommended by the International Humic Substances Society (Bai et al., 2015). The FA was stepwise eluted from an XAD-8 resin column into five sub-fractions: $FA_3$, $FA_5$, $FA_7$, $FA_9$, and $FA_{13}$ by use of pyrophosphate buffers with initial pHs of 3.0, 5.0, 7.0, 9.0 or 13.0 (Fig. S1) (Bai et al., 2015). The total phosphorous in FA sub-fractions was lower than 0.3% measured with molybdenum blue method after digesting at 110 °C and calculated as pyrophosphate (Bai et al., 2015).

Each FA sub-fraction was prepared at a concentration of 10.0 mg/L with 0.05 mol/L $KClO_4$ as background electrolyte. In details, the 100.0 mg FA sub-fractions were dissolved in water (about 100 mL), and then the solutions were filtered using a 0.22 μm membrane. The membranes were dried for 48 h at 45 °C before and after filtering the FA sub-fractions. The mass of non-soluble FA sub-fractions was calculated by the mass difference of the membranes subsequently, the dissolved FA sub-fractions were evaluated by reducing the weight of non-soluble FA sub-fractions from total weight. The filtered FA sub-fraction solutions were then diluted with $KClO_4$ solution to 10.0 mg/L as stock solutions (Bai et al., 2015). The pH values of solutions were controlled sequentially at 0.5 pH units from 2.5 to 11.5 by adding small amounts of $HClO_4$ or KOH. Each solution was continuously stirred by magnetic stirrer during fluorescence titration. All the solutions were purged for 15 min using nitrogen to avoid static quenching caused by oxygen and buffering effect of carbonate species during fluorescence spectra detection (Ryan and Weber, 1982). All chemicals were analytical reagent grade unless otherwise noted. All solutions were prepared in Milli-Q water then filtered through 0.45 μm filter membranes (Whatman, UK) before use.

### 2.2. Fluorescence spectral analysis

Fluorescence spectra of sub-fractions were measured using a fluorescence spectrometer (Hitachi F-7000, Tokyo, Japan) with a 1 cm path-length quartz cuvette at room temperature. EEM spectra were obtained by subsequently scanning emission (Em) wavelengths from 250 to 550 nm and excitation (Ex) wavelengths from 200 to 450 nm, both stepped by 2 nm intervals. Slit widths were 5 nm for both Ex and Em and scanning speed was set at 2400 nm·$min^{-1}$.

### 2.3. Parallel factor analysis

The three-way data of EEMs can be statistically reduced into trilinear terms and a residual array by using PARAFAC modeling (Stedmon and Bro, 2008) (Eq. (1)).

$$x_{ijg} = \sum_{n=1}^{N} a_{if} b_{jf} c_{gf} + \varepsilon_{ijg}, i = 1, .I; j = 1.J; g = 1, \ldots, G \quad (1)$$

where: for EEM data, $x_{ijg}$ represents fluorescence intensity of the i*th* sample measured at g*th* Ex wavelength and j*th* Em wavelength. Parameters *a*, *b*, and *c* represent concentration, Em spectra, and Ex spectra of fluorophores, respectively. *N* is the number of components and *f* represents the individual component in the samples. The $\varepsilon_{ijg}$ represents variability unexplained by the model.

PARAFAC modeling was separately performed on five sets of EEMs (19 samples for $FA_3$, $FA_9$ and $FA_{13}$, respectively; 16 samples for $FA_5$ and $FA_7$, respectively) for the $FA_3$-$FA_{13}$ at various pH values by utilizing the DOMFluor (version 1.7) toolbox in MATLAB software (Stedmon and Bro, 2008). In addition, several important preprocessing steps were applied to minimize the effects of scatter lines of the EEMs. The EEMs of the $KClO_4$ blank were subtracted from each sample EEMs. The region of no fluorescence (Ex ≪ Em) were inserted a series of zero values. The residual Rayleigh and Raman scatters were regulated using interpolation methods derived from Bahram et al. (2006) (Bahram et al., 2006; Maqbool and Hur, 2016; Wu et al., 2011; Xu et al., 2013; Yu et al., 2010a). The PARAFAC models with 2–7 components were computed

for the EEMs. Ex and Em loadings were constrained non-negative values (Lee et al., 2015; Maqbool and Hur, 2016; Murphy et al., 2013). The maximum fluorescence intensity ($F$) derived by use of the PARAFAC decomposition method, represented the relative concentration or intensity of the PARAFAC component (Maqbool and Hur, 2016).

### 2.4. Determination of dissociation constant

Binding parameters based on EEMs were successfully obtained to characterize interactions between DOM and environmental contaminants (Avendano et al., 2016; Cabaniss, 2002; Cabaniss and Shuman, 2002; Guo et al., 2015; Yamashita and Jaffé, 2008). Also, a 1:1 stoichiometric model has been employed previously to describe binding affinities between DOM and proton, as well as metal ions (e.g., $Cu^{2+}$, $Mn^{2+}$, $Co^{2+}$) (Midorikawa and Tanoue, 1998; Ryan et al., 1983; Ryan and Weber, 1982; Wu and Tanoue, 2001). Therefore, values for $pK_{a1}$ and $pK_{a2}$, calculated from reactions between PARAFAC components ($L$) and proton ($H$) at acidic or basic pH range, respectively, can be quantitatively described with 1:1 stoichiometric model (Eq. (2)).

$$log\frac{F_{H-pH}-F}{F-F_{L-pH}} = pK_a - \mathrm{pH} \quad (2)$$

where: quantities $F_{H\text{-}pH}$ and $F_{L\text{-}pH}$ obtained from MATLAB software fitting were $F$ at the high and low values of pH in specific pH ranges, respectively. The $pK_{a1}$ and $pK_{a2}$ values were calculated with MATLAB software at acidic and basic pH range, respectively (detailed derivational information of Eq. (2) see Supporting Information Appendices A and B).

## 3. Results and discussion

### 3.1. General EEM fluorescence spectral of FA sub-fractions

EEMs have been provided for compositions of FA, associated with humic-like, fulvic-like, protein-like substances (Chen et al., 2003; Sun et al., 2016). EEMs and spectral parameters of FA sub-fractions are shown (Table 1 and Fig. 1). For EEMs of $FA_3$ and $FA_5$ at pH 3.0, two main peaks were observed at Ex/Em wavelengths of 290–320/410–450 nm (Peak A) and 230–270/400–450 nm (Peak B) (Fig. 1 a1 and b1). Peak B of $FA_3$ tended to be resolved into two peaks at neutral (i.e. pH 7.0) or basic conditions (i.e. pH 11.0) (Table 1 and Fig. 1a2–a3). Three main peaks including Peak A, Peak B and Peak C (Ex/Em: 220–235/400–420 nm), were observed in EEMs of $FA_7$ at pH 3.0 (Fig. 1c1). Peaks B and C of $FA_7$ tended to merge into a single peak under basic conditions (i.e. pH 11.0) (Table 1 and Fig. 1c3). Peak D (Ex/Em: 260–275/310–320 nm) and weaker, less distinct peaks appeared at pH 5.0–9.0 for the EEMs of $FA_7$. The similar four peaks for $FA_7$ at pH 5.0–9.0 have been reported previously (Bai et al., 2015). Four peaks, Peak A, B, D and E (Ex/Em: 215–225/300–310 nm), were identified from the EEMs of $FA_9$ and $FA_{13}$ (Fig. 1d1–d3, e1–e3). Peak D and Peak E of $FA_9$ and $FA_{13}$ disappeared at basic pH range (i.e. pH 10.5–11.5). In addition, Peak B was broken into two peaks for $FA_{13}$ under basic conditions (i.e. pH 10.0–11.5) (Table 1 and Fig. 1d3, e3). The splitting of peaks ($FA_3$ and $FA_{13}$) and merging of peaks ($FA_7$) might be associated to the red/blue shifts of peaks and the various affinities of FA sub-fractions to proton (Chen et al., 2002; Wang et al., 2009). These phenomena should be investigated in the further study.

More detailed analyses showed that the Ex/Em of peak A of $FA_3$ was 10–19/13–29 nm longer than that of $FA_{13}$, and the Em of peak B of $FA_3$ was 6–27 nm longer than that of $FA_{13}$ for corresponding pH values (Table 1). The longer Ex and Em observed were related to greater amounts of conjugated aromatic $\pi$-electron systems with electron-withdrawing groups, such as carbonyl containing substituents and carboxyl constituents (Chen et al., 2002; Senesi et al., 1991; Wang et al., 2009). These results observed and presented here were consistent with the results of NMR analysis in previous study, indicating that $FA_3$ contained more carbonyl/carboxyl groups than did $FA_{13}$ (Bai et al., 2015).

Shifts in locations of peaks were complicated with changes in pH. With pH increasing from 3.0 to 11.0, blue shifts were observed for Peak A of $FA_3$ (Ex for 9 nm and Em for 7 nm), Peak A of $FA_7$ and $FA_9$ (both Ex for 7 nm), Peak B of $FA_3$ (Ex for 22 nm and Em for 4 nm), Peak B of $FA_9$ (Ex for 6 nm) and $FA_{13}$ (Ex for 6 and 32 nm); while red shifts were observed for Peak A of $FA_7$ (Em for 5 nm), Peak A of $FA_9$ (Em for 13 nm), Peak B of $FA_9$ (Em for 22 nm), Peak A of $FA_{13}$ (Em for 7 nm) and Peak B of $FA_{13}$ (Em for 9 and 19 nm) (Table 1). These inconsistent shifts of peaks were likely related to conformational changes of compositions for FA sub-fractions at various pH values. Red and blue shifts were also observed for EEMs of standard HAs from the International Humic Substance Society and extracellular polymeric substances as a function of pH (Mobed et al., 1996; Sheng and Yu, 2006). Maximum peak intensities were observed under neutral conditions (Table 1).

### 3.2. PARAFAC analysis of FA sub-fractions

Spectra of individual components were successfully deconvoluted by use of PARAFAC analysis on the EEMs of each sub-fraction at various pH values. Appropriate numbers of individual components were identified by PARAFAC models residual analysis and split half analysis (Fig. S2) (Maqbool and Hur, 2016; Stedmon and Bro, 2008; Wu et al.,

**Table 1**
Fluorescence spectral parameters of FA sub-fractions at pH 3.0, 7.0 and 11.0.

| Samples | pH | Peak A | | Peak B | | Peak C | | Peak D | | Peak E | |
|---|---|---|---|---|---|---|---|---|---|---|---|
| | | Ex/Em | Int.[a] | Ex/Em | Int.[a] | Ex/Em | Int.[a] | Ex/Em | Int.[a] | Ex/Em | Int.[a] |
| $FA_3$ | 3.0 | 319/442 | 314.0 | 258/440 | 408.2 | – | – | – | – | – | – |
| | 7.0 | 310/433 | 419.0 | 261/439 (230/434) | 578.4 (601.2) | – | – | – | – | – | – |
| | 11.0 | 310/435 | 362.5 | 259/438 (236/436) | 524.6 (533.7) | – | – | – | – | – | – |
| $FA_5$ | 3.0 | 308/430 | 226.2 | 259/427 | 340.0 | – | – | – | – | – | – |
| | 7.0 | 306/426 | 282.0 | 255/432 | 397.6 | – | – | – | – | – | – |
| | 11.0 | 305/428 | 223.2 | 255/429 | 334.7 | – | – | – | – | – | – |
| $FA_7$ | 3.0 | 309/413 | 225.4 | 266/406 | 410.3 | 229/408 | 426.5 | – | – | – | – |
| | 7.0 | 301/419 | 293.7 | 254/421 | 428.8 | 228/420 | 459.9 | – | – | – | – |
| | 11.0 | 302/418 | 255.0 | – | – | 228/419 | 432.6 | – | – | – | – |
| $FA_9$ | 3.0 | 307/415 | 169.0 | 261/413 | 252.8 | – | – | 270/315 | 193.9 | 215/300 | 177.6 |
| | 7.0 | 290/415 | 223.6 | 250/423 | 288.0 | – | – | 264/312 | 430.1 | 218/300 | 384.3 |
| | 11.0 | 300/428 | 197.0 | 255/435 | 280.0 | – | – | – | – | – | – |
| $FA_{13}$ | 3.0 | 300/413 | 191.4 | 262/413 | 254.7 | – | – | 272/316 | 187.3 | 220/308 | 155.5 |
| | 7.0 | 300/415 | 236.8 | 266/414 | 292.5 | – | – | 270/319 | 198.3 | 222/309 | 189.0 |
| | 11.0 | 300/420 | 169.7 | 256/432 (230/422) | 260.4 (270.7) | – | – | – | – | – | – |

– data not available.
[a] Int.: fluorescence intensity with arbitrary unit (a.u.).

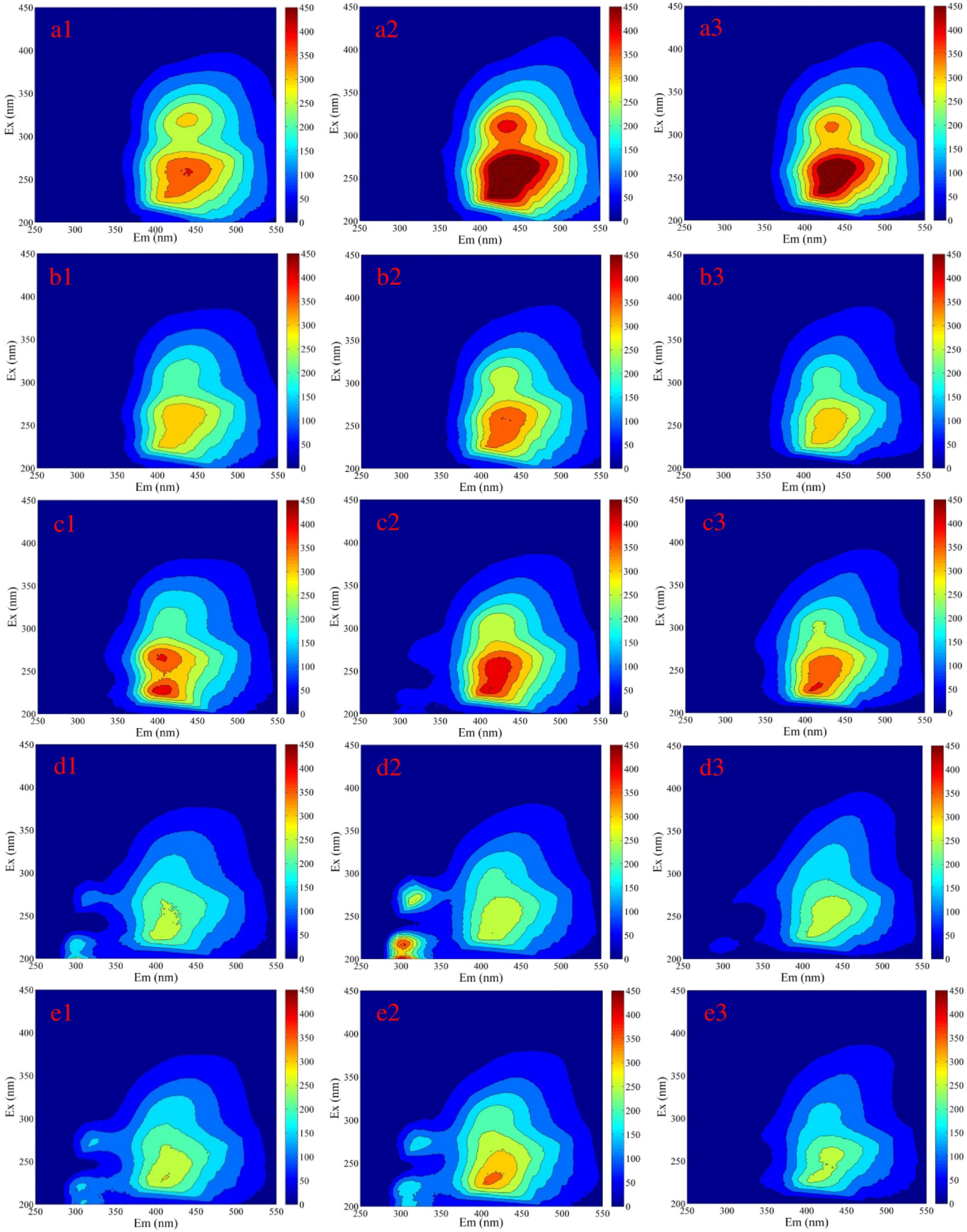


**Fig. 1.** Fluorescence EEMs of FA sub-fractions with arbitrary unit at pH 3.0, 7.0 and 11.0: $FA_3$ (a1–a3); $FA_5$ (b1–b3); $FA_7$ (c1–c3); $FA_9$ (d1–d3); $FA_{13}$ (e1–e3).

2011; Xu et al., 2013; Yu et al., 2010a). The residual analysis and split half analysis have been widely used to determine the appropriate numbers of PARAFAC components derived from DOM (Wu et al., 2011; Xu et al., 2013). Three PARAFAC components were determined for $FA_3$, $FA_5$ and $FA_7$, and four PARAFAC components were identified for $FA_9$ and $FA_{13}$ (Figs. 2 and S3).

Distributions of locations of peaks, component categories and primary compounds of PARAFAC components are shown (Table 2). Individual components identified by use of PARAFAC analysis were referred as Component 1 (C1, Ex/Em: 225–305/410–425 nm), Component 2 (C2, Ex/Em: 210–360/465–485 nm), Component 3 (C3, Ex/Em: 210–330/300–455 nm) and Component 4 (C4, Ex/Em: 220–275/320–325 nm) (Table 2). Based on distributions of Ex/Em of PARAFAC components reported previously (Chen et al., 2003; Wei et al., 2016; Zhang et al., 2011), the C1 ($FA_3$-$FA_{13}$), C2 ($FA_3$-$FA_{13}$) and C3 ($FA_3$-$FA_7$) were categorized as fulvic-like components, and C3 and C4 of both $FA_9$ and $FA_{13}$ were categorized as protein-like components (Table 2).

Values of *F* for each PARAFAC component at various pH values are presented (Figs. 3 and S4). For C1 ($FA_3$-$FA_{13}$), C2 ($FA_3$, $FA_7$ and $FA_{13}$) and C3 ($FA_3$) among fulvic-like components, *F* values were directly proportional to pH in the range of 2.5–4.5 and reached a plateau at pH 4.5–9.5, then were inversely proportional to pH in the range of 10.0–11.5. The rapid increase and decrease of fluorescence intensities at certain pH ranges were also reported during measurements of fluorescence titration of DOM (Midorikawa and Tanoue, 1998; Wu and Tanoue, 2001; Yan et al., 2013). Due to deprotonation of carboxylic-like and phenolic-like chromophores, intensity of fluorescence increased from pH 2.0 to 5.0 then decreased from 8.0 to 10.0 (Midorikawa and Tanoue, 1998; Wu and Tanoue, 2001; Yan et al., 2013). Therefore, increasing values of *F* at pH 2.5–4.5 were attributed to deprotonation of carboxylic-like chromophores, and decreasing values of *F* values at pH 10.0–11.5 were due to ionization of phenolic-like chromophores of fulvic-like components. According to the theory of Yan et al. (2013), C1 ($FA_3$-$FA_{13}$), C2 ($FA_3$, $FA_7$ and $FA_{13}$) and C3 ($FA_3$) were primarily composed of both carboxylic-like and phenolic-like chromophores (Table 2). Based on acid-basic properties, the same primary compounds were also reported for Suwannee River FA and Nordic Reservoir DOM (Midorikawa and Tanoue, 1998; Wu and Tanoue, 2001; Yan et al., 2013). The *F* values increased insignificantly as pH was increased from 2.5 to 8.0, and then decreased rapidly as pH was increased from 8.5 to 11.5 for C3 ($FA_5$). It can thus be speculated that C3 ($FA_5$) was primarily composed of phenolic-like chromophores. Values of *F* of C2 ($FA_5$ and $FA_9$) increased at pH values between 2.5 and 4.5, but exhibited less clear transitions at basic ranges (Fig. 3). Thus, C2 ($FA_5$ and $FA_9$) was primarily composed of carboxylic-like chromophores. C3 of $FA_7$ was composes of other unknown compounds, which were also reported previously (Yan et al., 2013) (Fig. S4).

For protein-like components, values of *F* of both C3 and C4 of $FA_9$ exhibited four stages with pH 2.5–11.5, including a plateau at pH 2.5–3.5, a rapid increasing at pH 3.5–5.5, a plateau at pH 5.5–8.5, and a decreasing at pH 8.5–11.5 (Fig. 3). Values of *F* values for both C3 and C4 of $FA_{13}$ increased insignificantly at pH 2.5–8.5, and then decreased rapidly at pH 8.5–11.5 (Fig. S4). The C3 and C4 ($FA_9$ and $FA_{13}$) were likely associated to peptide bond of protein-like components. The insignificant

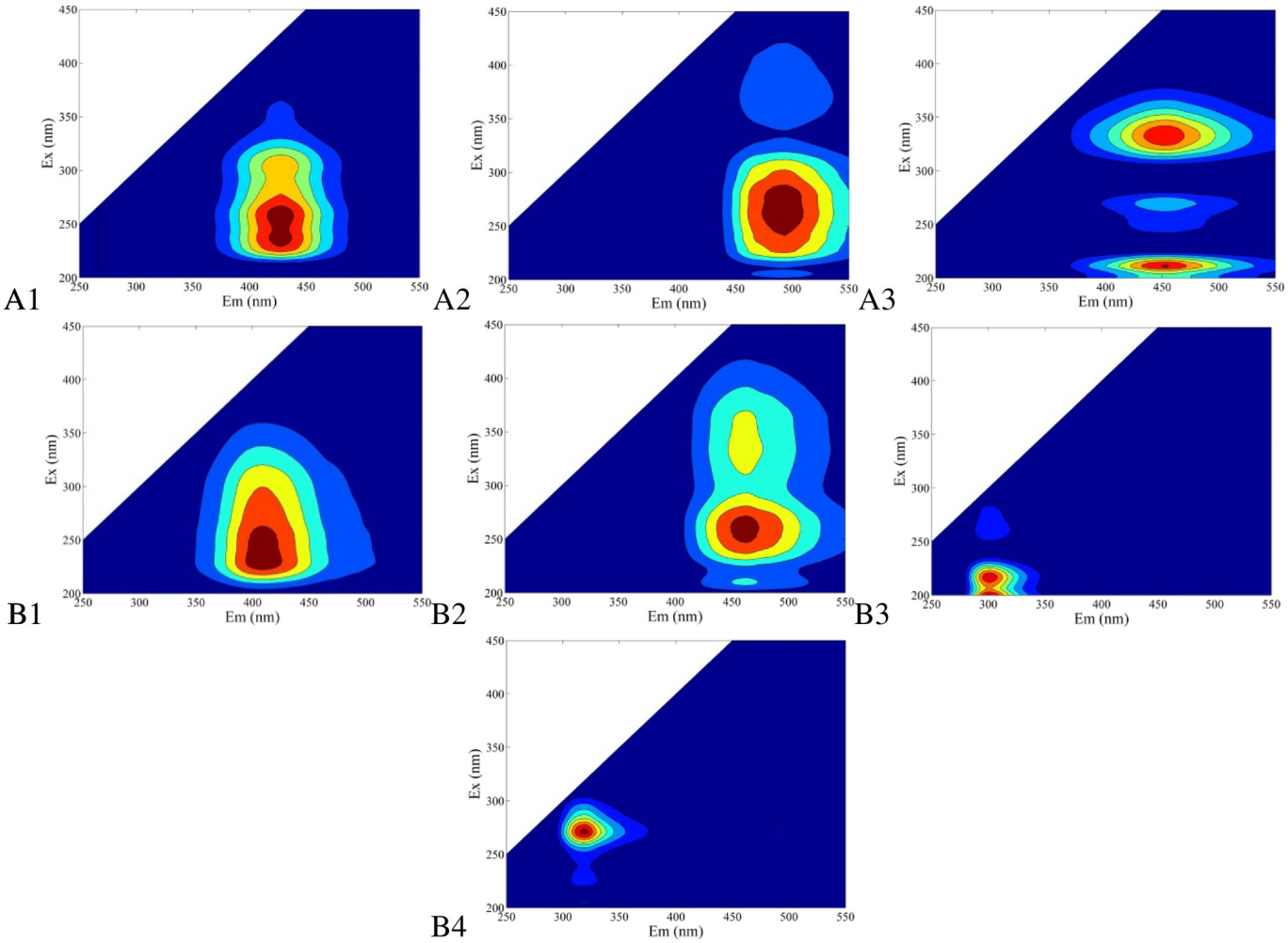


**Fig. 2.** Identified PARAFAC components of $FA_3$ and $FA_9$ with arbitrary unit: $FA_3$ (A1–A3); $FA_9$ (B1–B4).

**Table 2**
Summary of fluorescence parameters of PARAFAC components.

| Components | | Ex/Em locations | Component categories | Primary compounds in term of acid-base properties |
|---|---|---|---|---|
| $FA_3$ | C1 | (235,265,300) nm/425 nm | Fulvic-like | Carboxylic-like and phenolic-like |
| | C2 | (265,360 nm)/485 nm | Fulvic-like | Carboxylic-like and phenolic-like |
| | C3 | (210,260,330) nm/450 nm | Fulvic-like | Carboxylic-like and phenolic-like |
| $FA_5$ | C1 | (240,305 nm)/425 nm | Fulvic-like | Carboxylic-like and phenolic-like |
| | C2 | (210,250,350 nm)/475 nm | Fulvic-like | Carboxylic-like |
| | C3 | (210,255 nm)/455 nm | Fulvic-like | Phenolic-like |
| $FA_7$ | C1 | (225,255,300 nm)/410 nm | Fulvic-like | Carboxylic-like and phenolic-like |
| | C2 | (210,250,300 nm)/465 nm | Fulvic-like | Carboxylic-like and phenolic-like |
| | C3 | (225,260 nm)/405 nm | Fulvic-like | Other components |
| $FA_9$ | C1 | 225 nm/410 nm | Fulvic-like | Carboxylic-like and phenolic-like |
| | C2 | (210,260,340 nm)/465 nm | Fulvic-like | Carboxylic-like |
| | C3 | 220 nm/300 nm | Protein-like | Protein-like |
| | C4 | 275 nm/325 nm | Protein-like | Protein-like |
| $FA_{13}$ | C1 | (235,280 nm)/415 nm | Fulvic-like | Carboxylic-like and phenolic-like |
| | C2 | (210,265,350 nm)/470 nm | Fulvic-like | Carboxylic-like and phenolic-like |
| | C3 | (230,275 nm)/325 nm | Protein-like | Protein-like |
| | C4 | 220 nm/320 nm | Protein-like | Protein-like |

increasing *F* values of C3 and C4 for $FA_{13}$ indicated that $FA_{13}$ contained lesser amounts of carboxylic-like chromophores than $FA_9$, which was consistent with recent results detected by NMR analysis (Bai et al., 2015). Also, for the *F* values C3 and C4 of $FA_9$, the plateau stage (pH 2.5–3.5) was also observed in changes of fluorescence peak intensities with pH changing reported by Midorikawa and Tanoue (1998) (Fig. 3). The *F* values of C1 ($FA_3$ and $FA_9$), C2 ($FA_3$), C3 ($FA_9$) and C4 ($FA_9$) at pH 7.0 were lower than that on both sides. This phenomena was also observed by Sheng and Yu (2006) (Fig. 3), and it should to be further researched.

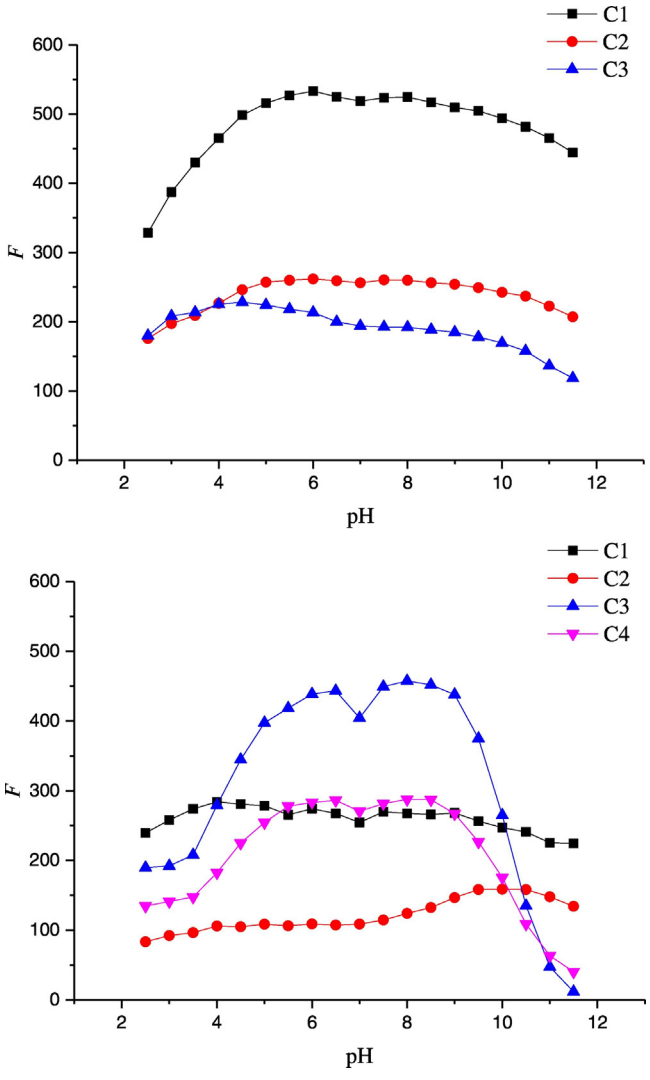


**Fig. 3.** *F* values of each PARAFAC component with arbitrary unit at various pH values for $FA_3$ (top) and $FA_9$ (bottom).

### 3.3. Determination of dissociation constants of PARAFAC components

The $pK_a$ of FA-proton had previously been determined by use of fluorescence titration at acidic pH (Midorikawa and Tanoue, 1998; Wu and Tanoue, 2001), however $pK_a$ values of PARAFAC components with protons have not been investigated. The *F* values of PARAFAC components at acidic and basic pH ranges were fitted by Eq. (2), respectively ($R^2$ = 0.97–0.99). The $pK_{a1}$ and $pK_{a2}$ values of PARAFAC components with protons ranged from 2.43 to 4.22 and 9.77 to 11.27, respectively (Table 3).

At acidic pH, $pK_{a1}$ values of fulvic-like components (2.43–4.13) were comparable to that of FA-proton (2.28–4.42) based on fluorescence peak intensities (Midorikawa and Tanoue, 1998; Wu and Tanoue, 2001). The $pK_{a1}$ values of fulvic-like components were also close to those of di-carboxylate molecules (2.5–4.3), except for maleic acid (Martell and Smith, 1975; Smith and Martell, 1989). These results indicated that fulvic-like components were likely predominated by di-carboxylate functional groups. Moreover, conditional stability constants for PARAFAC components of DOM for Cu(II), Cd(II) and Hg(II), as determined by use of the Ryan-Weber equation, were 4.48–6.32, 4.64–5.10 and 3.92–6.76, respectively (Guo et al., 2015; Wu et al., 2011; Yamashita and Jaffé, 2008). The lower $pK_{a1}$ values for binding of protons to fulvic-like components suggested that protons were bound relatively weaker than were some specific metal ions. At basic pH, $pK_{a2}$ values of fulvic-like components were in the range of 9.95–11.27, which were similar to those of hydroxybenzenes, which had a range of 8.0–10.0 (Midorikawa and Tanoue, 1998). This result indicated that the phenolic groups in fulvic-like components were likely to play a major role in binding of protons by FA at basic pH. The conditional stability constants value of the second ligand class in DOM (~9.0), which was obtained using fluorescence quenching titration with Cu(II) at pH 8.15 (Midorikawa and Tanoue, 1998), was lesser than $pK_{a2}$ values of fulvic-like components.

DOM with greater contents of carboxyl-like chromophores exhibited lesser $pK_{a1}$ values for protons (Midorikawa and Tanoue, 1998). Therefore, for fulvic-like components, the C1 ($FA_3$, $FA_5$, $FA_9$ and $FA_{13}$), C2 ($FA_5$-$FA_{13}$) and C3 ($FA_3$) exhibited lesser $pK_{a1}$ values (2.43–3.40), which indicated more carboxyl-like chromophores. In addition, the C1 ($FA_9$ and $FA_{13}$) and C3 ($FA_5$) among fulvic-like components with lesser $pK_{a2}$ values (9.95–10.12) suggested greater content of phenolic-like chromophores. These conclusions were consistent with the results of

**Table 3**
Dissociation constants of PARAFAC components at acidic and basic pH.

| Components | | At acidic pH range | | | | | | At basic pH range | | | | | |
|---|---|---|---|---|---|---|---|---|---|---|---|---|---|
| | | $F_{pH\text{-}max}$[a] | $F_{pH\text{-}min}$[b] | $F_{H\text{-}pH}$ | $F_{L\text{-}pH}$ | $pK_{a1}$ | $R^2$ | $F_{pH\text{-}max}$[a] | $F_{pH\text{-}min}$[b] | $F_{H\text{-}pH}$ | $F_{L\text{-}pH}$ | $pK_{a2}$ | $R^2$ |
| $FA_3$ | C1 | 527.0 | 328.6 | 518.8 | 314.4 | 3.40 | 0.9817 | 509.5 | 444.4 | 508.2 | 434.6 | 10.77 | 0.9884 |
| | C2 | 259.8 | 175.6 | 260.1 | 177.2 | 3.74 | 0.9812 | 254.1 | 207.0 | 251.9 | 196.3 | 10.91 | 0.9855 |
| | C3 | 228.3 | 179.8 | 226.9 | 125.5 | 2.43 | 0.9705 | 184.7 | 118.5 | 183.2 | 107.1 | 10.77 | 0.9938 |
| $FA_5$ | C1 | 349.7 | 294.2 | 344.4 | 280.7 | 3.02 | 0.9668 | 337.6 | 287.3 | 335.3 | 259.9 | 11.27 | 0.9836 |
| | C2 | 108.7 | 87.9 | 107.7 | 79.2 | 2.84 | 0.9863 | 104.7 | 79.9 | + | + | + | + |
| | C3 | 128.0 | 117.6 | + | + | + | + | 104.3 | 12.5 | 113.6 | 0 | 10.08 | 0.9994 |
| $FA_7$ | C1 | 386.7 | 36.1 | 395.2 | 19.1 | 4.13 | 0.9902 | 394.8 | 342.2 | 395.9 | 340.2 | 10.32 | 0.9945 |
| | C2 | 209.4 | 176.4 | 207.8 | 158.4 | 2.75 | 0.9705 | 226.6 | 172.4 | 228.2 | 160.3 | 10.88 | 0.9865 |
| | C3 | 379.3 | 17.9 | + | + | + | + | 16.7 | 0 | + | + | + | + |
| $FA_9$ | C1 | 284.2 | 239.6 | 289.5 | 222.3 | 2.95 | 0.9995 | 268.2 | 224.2 | 268.8 | 222.4 | 10.12 | 0.9654 |
| | C2 | 108.5 | 83.2 | 108.0 | 78.7 | 3.17 | 0.9678 | 158.8 | 134.1 | + | + | + | + |
| | C3 | 418.3 | 189.7 | 432.6 | 178.5 | 4.22 | 0.9965 | 437.8 | 11.6 | 472.6 | 0 | 10.10 | 0.9995 |
| | C4 | 277.7 | 134.5 | 285.4 | 132.1 | 3.33 | 0.9977 | 267.0 | 40.2 | 279.8 | 32.3 | 10.13 | 0.9983 |
| $FA_{13}$ | C1 | 307.0 | 240.4 | 303.2 | 214.5 | 2.89 | 0.9744 | 287.6 | 220.3 | 293.7 | 220.6 | 9.95 | 0.9942 |
| | C2 | 109.3 | 88.0 | 108.7 | 82.9 | 3.07 | 0.9738 | 152.9 | 108.8 | 155.0 | 102.2 | 10.71 | 0.9946 |
| | C3 | 177.5 | 157.7 | + | + | + | + | 145.8 | 30.4 | 164.5 | 25.4 | 9.77 | 0.9904 |
| | C4 | 135.2 | 115.2 | + | + | + | + | 115.6 | 6.62 | 128.9 | 0 | 10.02 | 0.9936 |

+ data cannot be accurately estimated.
[a] $F_{pH\text{-}max}$: the maximum *F* values with arbitrary unit of individual components derived from PARAFAC in specific pH range.
[b] $F_{pH\text{-}min}$: the minimum *F* values with arbitrary unit of individual components derived from PARAFAC in specific pH range.

primary compounds of PARAFAC components in term of acid-base properties (Table 2).

At acidic pH, $pK_{a1}$ values of protein-like components (3.33–4.22) were greater than the $pK_a$ values of amino acids (1.9–2.4) (Midorikawa and Tanoue, 1998). The high $pK_{a1}$ values of protein-like components might be due to less clustered carboxyl groups existing in aliphatic, alicyclic structures (Leenheer et al., 2003). At basic pH, $pK_{a2}$ values of protein-like components (9.77–10.13) were similar to $pK_a$ values of amino acids (9.61–12.02) (Aliyu and Na'Aliya, 2009). These results indicated that amino acid groups in PARAFAC components were significant factors in FA-proton binding at basic pH.

The $pK_{a1}$ values of C3 ($FA_5$, $FA_7$, and $FA_{13}$) and C4 ($FA_{13}$), as well as $pK_{a2}$ values of C2 ($FA_5$ and $FA_9$) and C3 ($FA_7$) could not be accurately estimated because of smaller *F* transitions with pH increasing from 2.5 to 6.5 and pH decreasing from 7.5 to 11.5, respectively. The smaller *F* transitions were also consistent with the lower content of carboxylic-like or phenolic-like chromophores (Tables 2–3). The un-calculable $pK_{a1}$ values for both C3 and C4 of $FA_9$ indicated that the protein-like components of $FA_9$ presented less content of carboxylic-like chromophores than that of $FA_{13}$. EEM combined with a PARAFAC analysis is a useful tool for investigating the interaction mechanisms between FA sub-fractions and proton. This technique can be extended for the studies of FA derived from different sources with other chemical species.

## 4. Conclusions

Pattern of EEM of FA sub-fractions changed during fluorescence titration. Splitting of peak B (Ex/Em: 230–270/400–450 nm) of $FA_3$ and $FA_{13}$, merging of Peaks B and Peak C (Ex/Em: 220–235/400–420 nm) of $FA_7$, disappearance of Peak D (Ex/Em: 260–275/310–320 nm) and Peak E (Ex/Em: 215–225/300–310 nm) of both $FA_9$ and $FA_{13}$ were observed at pH ranging from 2.5 to 11.5. According to Yan's theory, the C1 ($FA_3$-$FA_{13}$), C2 ($FA_3$, $FA_7$, and $FA_{13}$) and C3 ($FA_3$) were categorized as fulvic-like components with primary compounds of both carboxylic-like and phenolic-like chromophores. The C2 ($FA_5$ and $FA_9$) and C3 ($FA_5$) were attributed to fulvic-like components with major compounds of carboxylic-like chromophores and phenolic-like chromophores, respectively. The C3 ($FA_9$ and $FA_{13}$) and C4 ($FA_9$ and $FA_{13}$) were primarily composed of protein-like components. The $pK_a$ values for fulvic-like components ranged from 2.43 to 4.13 and 9.95 to 11.27 at acidic and basic pH ranges, respectively. These results might be associated with protonation of di-carboxylate and phenolic functional groups in FA sub-fractions. The $pK_{a1}$ values (3.33–4.22) for protein-like components were 1–2 units greater than that of amino acids, which indicated fewer clustered carboxyl groups existing in aliphatic, alicyclic structures in FA sub-fractions. The $pK_{a2}$ values (9.77–10.13) for protein-like components were similar to those for amino acids at basic pH. Protein-like components in $FA_9$ contained more carboxyl groups than did $FA_{13}$.

## Acknowledgements

This work was financially supported by the National Natural Science Foundation of China (Nos. 41521003, 41630645, 41173084 and 41573130), Beijing Natural Science Foundation (8162044), Canada Research Chair program, Einstein Professor Program of the Chinese Academy of Sciences, and High Level Foreign Experts Program (#GDT20143200016).

## Appendix A. Supplementary data

Supplementary data to this article can be found online at http://dx.doi.org/10.1016/j.scitotenv.2017.06.164.

## References

Aliyu, H.N., Na'Aliya, J., 2009. Determination and stability constants of Manganese (II) amino acid complexes. Bay. J. Pure. Appl. Sci. 2, 191–193.
Avendano, L., Gledhill, M., Achterberg, E.P., Rerolle, V.M., Schlosser, C., 2016. Influence of ocean acidification on the organic complexation of iron and copper in Northwest European shelf seas; a combined observational and model study. Front. Mar. Sci. 58, 1–19.
Bahram, M., Bro, R., Stedmon, C., Afkhami, A., 2006. Handling of Rayleigh and Raman scatter for PARAFAC modeling of fluorescence data using interpolation. J. Chemom. 20, 99–105.
Bai, Y., Wu, F., Xing, B., Meng, W., Shi, G., Ma, Y., et al., 2015. Isolation and characterization of Chinese standard fulvic acid sub-fractions separated from forest soil by stepwise elution with pyrophosphate buffer. Sci Rep 5, 8723.
Bro, R., 1997. PARAFAC. Tutorial and applications. Chemom. Intell. Lab. Syst. 38, 149–171.
Cabaniss, S.E., 2002. Synchronous fluorescence spectra of metal-fulvic acid complexes. Environ. Sci. Technol. 26, 1133–1139.
Cabaniss, S.E., Shuman, M.S., 2002. Fluorescence quenching measurements of copper-fulvic acid binding. Anal. Chem. 60, 2418–2421.
Cai, D., Yang, X., Wang, S., Chao, Y., Morel, J.L., Qiu, R., 2016. Effects of dissolved organic matter derived from forest leaf litter on biodegradation of phenanthrene in aqueous phase. J. Hazard. Mater. 324, 516–525.
Chen, J., Gu, B., Leboeuf, E.J., Pan, H., Dai, S., 2002. Spectroscopic characterization of the structural and functional properties of natural organic matter fractions. Chemosphere 48, 59–68.
Chen, W., Westerhoff, P., Leenheer, J.A., Booksh, K., 2003. Fluorescence excitation — - emission matrix regional integration to quantify spectra for dissolved organic matter. Environ. Sci. Technol. 37, 5701–5710.

Cory, R.M., Mcknight, D.M., 2005. Fluorescence spectroscopy reveals ubiquitous presence of oxidized and reduced quinones in dissolved organic matter. Environ. Sci. Technol. 39, 8142–8149.
Dai, J., Ran, W., Xing, B., Gu, M., Wang, L., 2006. Characterization of fulvic acid fractions obtained by sequential extractions with pH buffers, water, and ethanol from paddy soils. Geoderma 135, 284–295.
Gao, Y., Yan, M., Korshin, G.V., 2015. Effects of ionic strength on the chromophores of dissolved organic matter. Environ. Sci. Technol. 49, 5905–5912.
Giesy, J., 1983. Metal binding capacity of soft, acid, organic-rich waters. Toxicol. Environ. Chem. 6, 203–224.
Giesy, J.P., Briese, L.A., Leversee, G.J., 1978. Metal binding capacity of selected Maine surface waters. Environ. Geol. 2, 257–268.
Giesy, J.P., Newell, A., Leversee, G.J., 1983. Copper speciation in soft, acid, humic waters: effects on copper bioaccumulation by and toxicity to *Simocephalus serrulatus* (Daphnidae). Sci. Total Environ. 28, 23–36.
Giesy, J.P., Geiger, R.A., Kevern, N.R., Alberts, J.J., 1986. $UO_2^{2+}$-humate interactions in soft, acid, humate-rich waters. J. Environ. Radioact. 4, 39–64.
Giesy, J.P., Alberts, J.J., Evans, D.W., 2010. Conditional stability constants and binding capacities for copper (II) by dissolved organic carbon isolated from surface waters of the southeastern United States. Environ. Toxicol. Chem. 5, 139–154.
Guo, X.J., Zhu, N.M., Chen, L., Yuan, D.H., He, L.S., 2015. Characterizing the fluorescent properties and copper complexation of dissolved organic matter in saline-alkali soils using fluorescence excitation-emission matrix and parallel factor analysis. J. Soils Sediments 15, 1473–1482.
He, X.S., Xi, B.D., Li, X., Pan, H.W., An, D., Bai, S.G., et al., 2013. Fluorescence excitation–emission matrix spectra coupled with parallel factor and regional integration analysis to characterize organic matter humification. Chemosphere 93, 2208–2215.
Kowalczuk, P., Durako, M.J., Young, H., Kahn, A.E., Cooper, W.J., Gonsior, M., 2009. Characterization of dissolved organic matter fluorescence in the South Atlantic Bight with use of PARAFAC model: interannual variability. Mar. Chem. 113, 182–196.
Lee, B.M., Seo, Y.S., Hur, J., 2015. Investigation of adsorptive fractionation of humic acid on graphene oxide using fluorescence EEM-PARAFAC. Water Res. 73, 242–251.
Leenheer, J.A., Wershaw, R.L., Brown, G.K., Reddy, M.M., 2003. Characterization and diagenesis of strong-acid carboxyl groups in humic substances. Appl. Geochem. 18, 471–482.
Lehmann, J., Kleber, M., 2015. The contentious nature of soil organic matter. Nature 528, 60–68.
Leversee, G.J., Landrum, P.F., Giesy, J.P., Fannin, T., 1983. Humic acids reduce bioaccumulation of some polycyclic aromatic hydroca. Can. J. Fish. Aquat. Sci. 40, 63–69.
Maqbool, T., Hur, J., 2016. Changes in fluorescent dissolved organic matter upon interaction with anionic surfactant as revealed by EEM-PARAFAC and two dimensional correlation spectroscopy. Chemosphere 161, 190–199.
Martell, A.E., Smith, R.M., 1975. Critical Stability Constants. 6 pp. 264–283.
Midorikawa, T., Tanoue, E., 1998. Molecular masses and chromophoric properties of dissolved organic ligands for copper(II) in oceanic water. Mar. Chem. 62, 219–239.
Mobed, J.J., Hemmingsen, S.L., Autry, J.L., Mcgown, L.B., 1996. Fluorescence characterization of IHSS humic substances: total luminescence spectra with absorbance correction. Environ. Sci. Technol. 30, 3061–3065.
Murphy, K.R., Stedmon, C.A., Graeber, D., Bro, R., 2013. Fluorescence spectroscopy and multi-way techniques. PARAFAC. Anal. Methods. 5, 38–65.
Pace, M.L., Reche, I., Cole, J.J., Fernández-Barbero, A., Mazuecos, I.P., Prairie, Y.T., 2012. pH change induces shifts in the size and light absorption of dissolved organic matter. Biogeochemistry 108, 109–118.
Piccolo, A., Conte, P., Cozzolino, A., 1999. Effects of mineral and monocarboxylic acids on the molecular association of dissolved humic substances. Eur. J. Soil Sci. 50, 687–694.
Romera-Castillo, C., Chen, M., Yamashita, Y., Jaffé, R., 2014. Fluorescence characteristics of size-fractionated dissolved organic matter: implications for a molecular assembly based structure? Water Res. 55, 40–51.
Ryan, D.K., Weber, J.H., 1982. Fluorescence quenching titration for determination of complexing capacities and stability constants of fulvic acid. Anal. Chem. 54, 986–990.
Ryan, D.K., Thompson, C.P., Weber, J.H., 1983. Comparison of $Mn^{2+}$, $Co^{2+}$, and $Cu^{2+}$ binding to fulvic acid as measured by fluorescence quenching. Can. J. Chem. 61, 1505–1509.
Senesi, N., Miano, T.M., Provenzano, M.R., Brunetti, G., 1991. Characterization, differentiation, and classification of humic substances by fluorescence spectroscopy. Soil Sci. 152, 248–252.
Sgroi, M., Roccaro, P., Korshin, G.V., Greco, V., Sciuto, S., Anumol, T., et al., 2016. Use of fluorescence EEM to monitor the removal of emerging contaminants in full scale wastewater treatment plants. J. Hazard. Mater. 323, 367–376.
Sheng, G.P., Yu, H.Q., 2006. Characterization of extracellular polymeric substances of aerobic and anaerobic sludge using three-dimensional excitation and emission matrix fluorescence spectroscopy. Water Res. 40, 1233–1239.
Smith, R.M., Martell, A.E., 1989. Critical stability constants. Vol. 2: Amines. Plenum Press, pp. 1–6.
Stedmon, C.A., Bro, R., 2008. Characterizing dissolved organic matter fluorescence with parallel factor analysis: a tutorial. Limnol. Oceanogr. Methods 6, 572–579.
Sun, J., Guo, L., Li, Q., Zhao, Y., Gao, M., She, Z., et al., 2016. Three-dimensional fluorescence excitation-emission matrix (EEM) spectroscopy with regional integration analysis for assessing waste sludge hydrolysis at different pretreated temperatures. Environ. Sci. Pollut. Res. Int. 24061–24067.
Timko, S.A., Gonsior, M., Cooper, W.J., 2015. Influence of pH on fluorescent dissolved organic matter photo-degradation. Water Res. 85, 266–274.
Tipping, E., 2005. Modelling Al competition for heavy metal binding by dissolved organic matter in soil and surface waters of acid and neutral pH. Geoderma 127, 293–304.
Wang, Z., Wu, Z., Tang, S., 2009. Characterization of dissolved organic matter in a submerged membrane bioreactor by using three-dimensional excitation and emission matrix fluorescence spectroscopy. Water Res. 43, 1533–1540.
Wang, J., Lü, C., He, J., Zhao, B., 2016. Binding characteristics of $Pb^{2+}$ to natural fulvic acid extracted from the sediments in Lake Wuliangsuhai, Inner Mongolia plateau, P. R. China. Environ. Earth Sci. 75, 1–11.
Wei, Z., Wang, X., Zhao, X., Xi, B., Wei, Y., Zhang, X., et al., 2016. Fluorescence characteristics of molecular weight fractions of dissolved organic matter derived from composts. Int. Biodeterior. Biodegrad. 113, 187–194.
Wu, F., Tanoue, E., 2001. Isolation and partial characterization of dissolved copper-complexing ligands in streamwaters. Environ. Sci. Technol. 35, 3646–3652.
Wu, J., Zhang, H., He, P.J., Shao, L.M., 2011. Insight into the heavy metal binding potential of dissolved organic matter in MSW leachate using EEM quenching combined with PARAFAC analysis. Water Res. 45, 1711–1719.
Xia, X.H., Li, G.C., Yang, Z.F., Chen, Y.M., Huang, G.H., 2009. Effects of fulvic acid concentration and origin on photodegradation of polycyclic aromatic hydrocarbons in aqueous solution: importance of active oxygen. Environ. Pollut. 157, 1352–1359.
Xu, H., Yu, G., Yang, L., Jiang, H., 2013. Combination of two-dimensional correlation spectroscopy and parallel factor analysis to characterize the binding of heavy metals with DOM in lake sediments. J. Hazard. Mater. 263, 412–421.
Yamashita, Y., Jaffé, R., 2008. Characterizing the interactions between trace metals and dissolved organic matter using excitation−emission matrix and parallel factor analysis. Environ. Sci. Technol. 42, 7374–7379.
Yan, M., Fu, Q., Li, D., Gao, G., Wang, D., 2013. Study of the pH influence on the optical properties of dissolved organic matter using fluorescence excitation-emission matrix and parallel factor analysis. J. Lumin. 142, 103–109.
Yu, G.H., Luo, Y.H., Wu, M.J., Tang, Z., Liu, D.Y., Yang, X.M., et al., 2010a. PARAFAC modeling of fluorescence excitation-emission spectra for rapid assessment of compost maturity. Bioresour. Technol. 101, 8244–8251.
Yu, H.B., Xi, B.D., Guo, X.J., He, X.S., Ma, W.C., Wei, Z.M., et al., 2010b. Relationship between humification and salinity of saline soils around lakes in arid and semi-arid regions by fluorescence spectroscopy. Fresenius Environ. Bull. 19, 1136–1143.
Yu, G.H., Wu, M.J., Luo, Y.H., Yang, X.M., Ran, W., Shen, Q.R., 2011. Fluorescence excitation-emission spectroscopy with regional integration analysis for assessment of compost maturity. Waste Manag. 31, 1729–1736.
Zhang, Y., Yin, Y., Feng, L., Zhu, G., Shi, Z., Liu, X., et al., 2011. Characterizing chromophoric dissolved organic matter in Lake Tianmuhu and its catchment basin using excitation-emission matrix fluorescence and parallel factor analysis. Water Res. 45, 5110–5122.

**Supporting Information**

# Interactions between stepwise-eluted sub-fractions of fulvic acids and protons revealed by fluorescence titration combined with EEM-PARAFAC

Fanhao Song[1], Fengchang Wu[1], Fei Guo[1], Hao Wang[1], Weiying Feng[1], Min Zhou[2], Yanghui Deng[1], Yingchen Bai[1*], Baoshan Xing[3], John P. Giesy[1,4]

[1]State Key Laboratory of Environmental Criteria and Risk Assessment, Chinese Research Academy of Environmental Science, Beijing, 10012, China

[2]School of Environmental and Municipal Engineering, Qingdao University of Technology, Qingdao, 266033, China

[3]Stockbridge School of Agriculture, University of Massachusetts, Amherst, MA, 01003, USA

[4]Department of Biomedical and Veterinary Biosciences and Toxicology Centre, University of Saskatchewan, Saskatoon, Saskatchewan, SK, S7N 5B3, Canada

Number of Pages (including this cover sheet): 9

Number of Figs.: 4

[*]Corresponding author: Tel.: +86-10-84931804; Fax: +86-10-84931804.

E-mail: baiyc@craes.org.cn.

## Supplementary caption

**Fig. S1.** Extraction and fractionation procedures of FA.

**Fig. S2.** Residual analysis and split half analysis for PARAFAC model validation for FA sub-fractions: $FA_3$:a1-a2; $FA_5$:b1-b2; $FA_7$:c1-c2; $FA_9$:d1-d2; $FA_{13}$:e1-e2.

**Fig. S3.** Identified PARAFAC components of $FA_5$, $FA_7$ and $FA_{13}$ with arbitrary unit: $FA_5$ (a1-a3); $FA_7$ (b1-b3); $FA_{13}$ (c1-c4).

**Fig. S4.** *F* values of each PARAFAC component with arbitrary unit at various pH values for $FA_5$, $FA_7$ and $FA_{13}$: $FA_5$ (top); $FA_7$ (middle); $FA_{13}$ (bottom).

**Appendix A and Appendix B.** Detailed derivational information of equation (2) in manuscript.

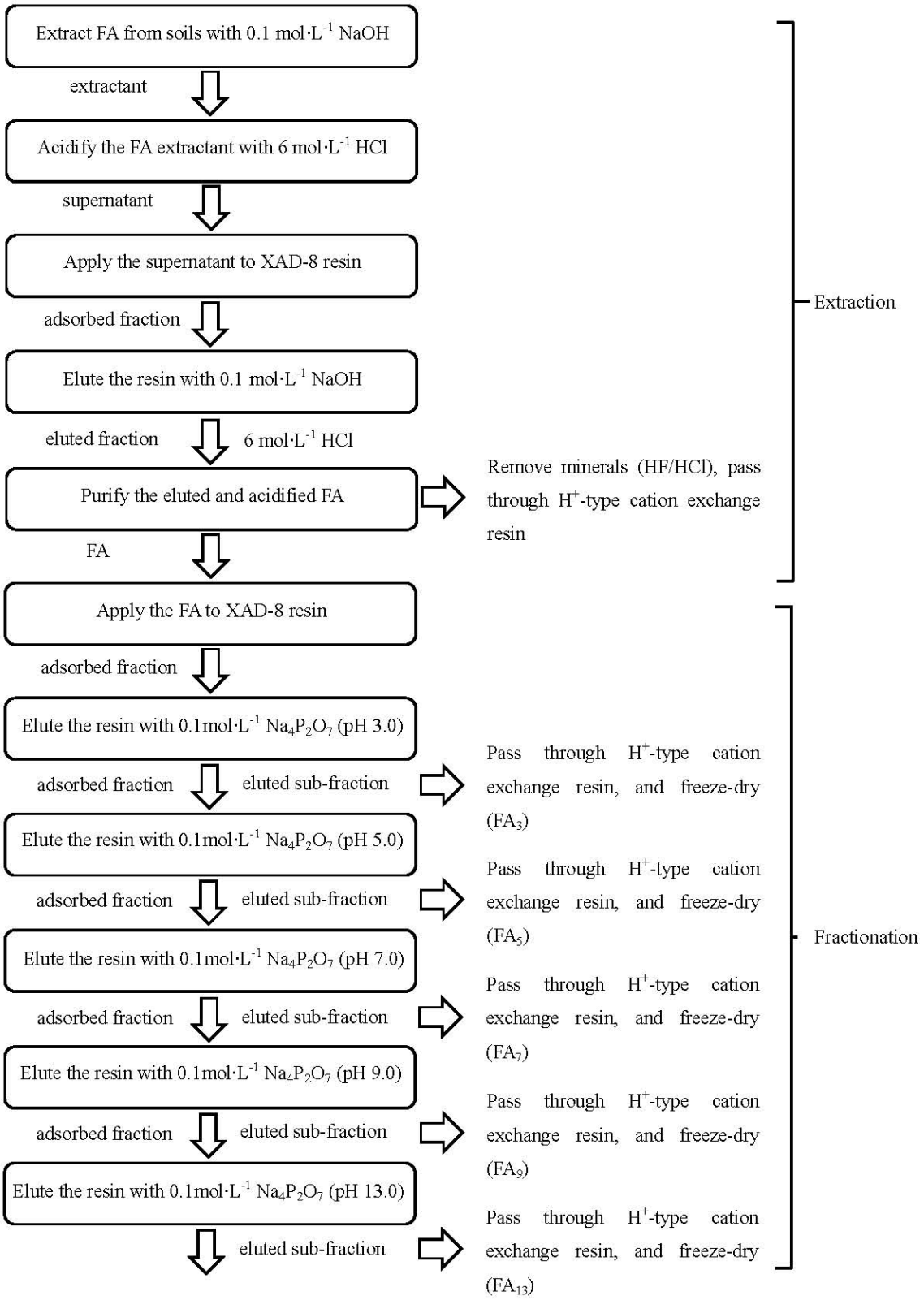


**Fig. S1.** Extraction and fractionation procedures of FA.

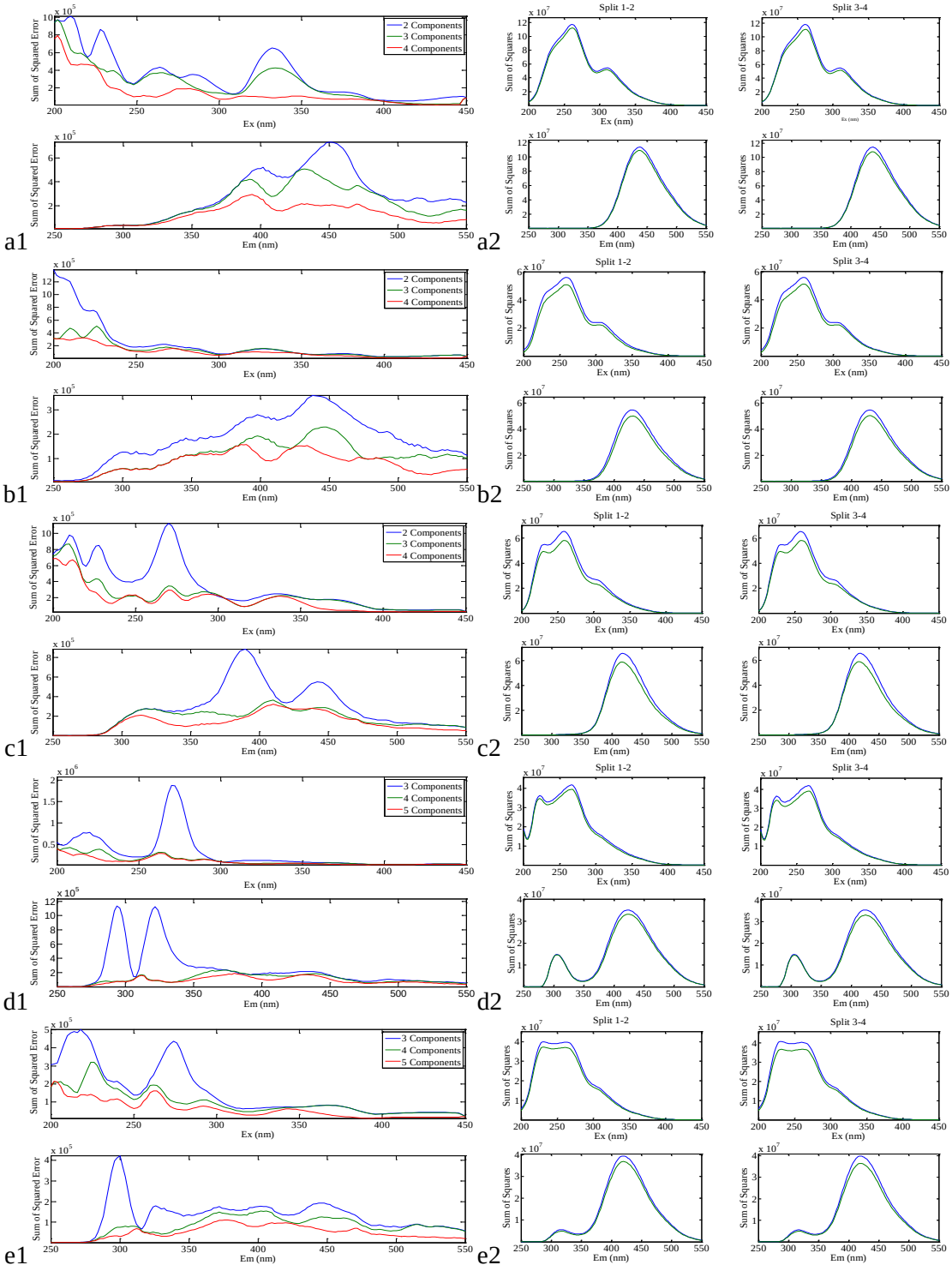


**Fig. S2.** Residual analysis and split half analysis for PARAFAC model validation for FA sub-fractions: $FA_3$:a1-a2; $FA_5$:b1-b2; $FA_7$:c1-c2; $FA_9$:d1-d2; $FA_{13}$:e1-e2.

For $FA_3$-$FA_7$, the residual analysis showed a great improvement of fit from two to three component model, while little enhancement was observed from three to four component model, indicating three components were adequate for these data (a1, b1, c1 in Fig. S2). For $FA_9$ and $FA_{13}$, the residual analysis showed a great improvement of fit from three to four component model, while little enhancement was observed from four to five component model, indicating four components were adequate for these data (d1, e1 in Fig. S2).

In addition, the similar curves of each pair of halves based on the split half analysis (a2, b2, c2, d2, e2 in Fig. S2) further validated that three was the appropriate number of components for $FA_3$-$FA_7$ and four was the appropriate number of components for $FA_9$ and $FA_{13}$.

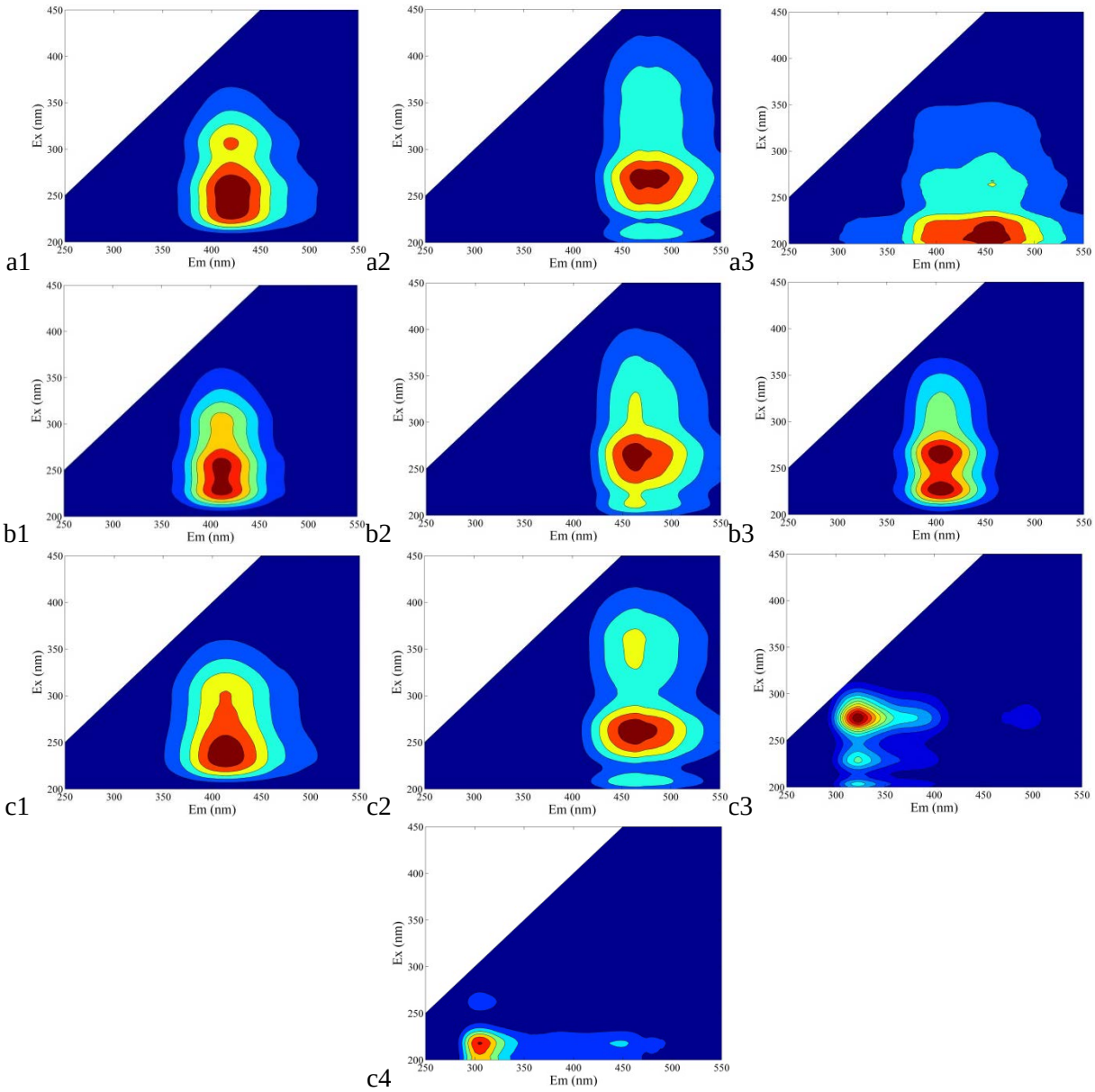


**Fig. S3.** Identified PARAFAC components of $FA_5$, $FA_7$ and $FA_{13}$ with arbitrary unit: $FA_5$ (a1-a3); $FA_7$ (b1-b3); $FA_{13}$ (c1-c4).

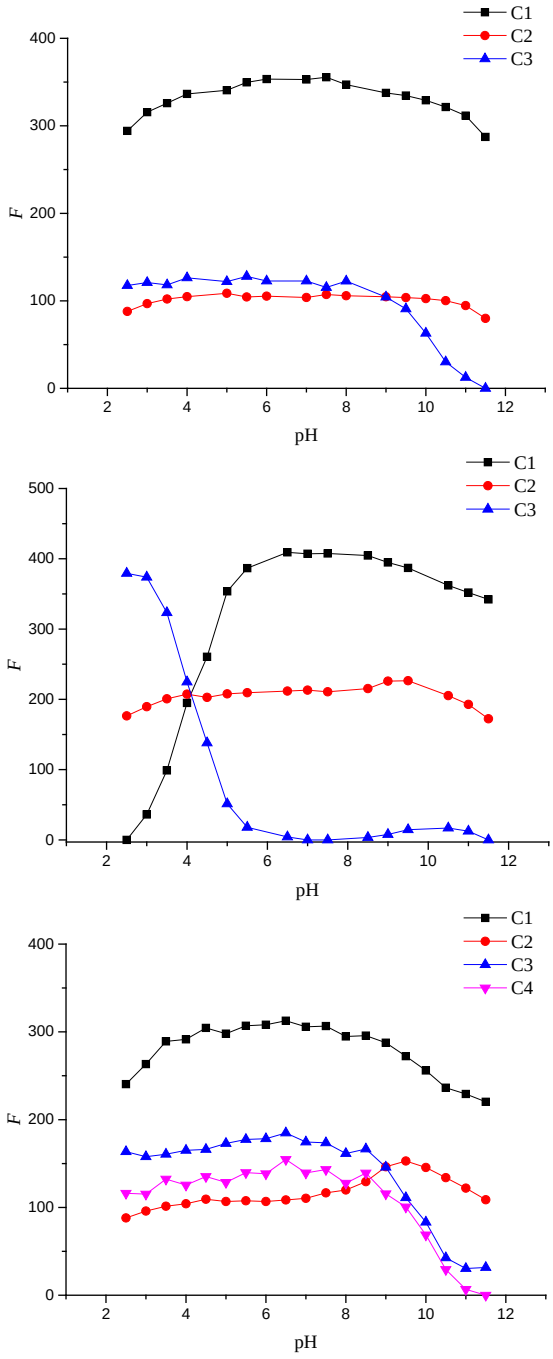


**Fig. S4.** *F* values of each PARAFAC component with arbitrary unit at various pH values for $FA_5$, $FA_7$ and $FA_{13}$: $FA_5$ (top); $FA_7$ (middle); $FA_{13}$ (bottom).

## Appendix A

Dissociation constants (p$K_{a1}$) of PARAFAC components were estimated from the increasing maximum fluorescence intensity ($F$) with the increase of pH at acid conditions. At acidic pH range, the reactions between PARAFAC component ($L_1$) and proton ($H$) can be quantitatively described with 1:1 stoichiometric model (Equations A1 and A2).

$$HL_1 \leftrightarrow L_1 + H \quad \text{A1}$$

The dissociation constant, $K_{a1}$, can be expressed:

$$K_{a1} = \frac{[L_1][H]}{[HL_1]} \quad \text{A2}$$

During fluorescence titration, the $F$ is associated with concentration ($C$) of PARAFAC component ($L_1$) by using the molar fluorescence coefficient ($\varepsilon$) (Equations A3-A5).

$$F_{H-pH} = \varepsilon_{L_1} \cdot C_{L_1} \quad \text{at high pH} \quad \text{A3}$$

$$F_{L-pH} = \varepsilon_{HL_1} \cdot C_{L_1} \quad \text{at low pH} \quad \text{A4}$$

$$F = \varepsilon_{L_1} \cdot [L_1] + \varepsilon_{HL_1} \cdot [HL_1] \quad \text{at middle pH} \quad \text{A5}$$

$F_{\text{H-pH}}$ is for $L_1$, dissociated at high pH; $F_{\text{L-pH}}$ is for $HL_1$, dissociated at a low pH.

From mass balance of $C_{L_1} = [L_1] + [HL_1]$,

$$F_{H-pH} - F = \left(\varepsilon_{L_1} - \varepsilon_{HL_1}\right) \cdot [HL_1] \quad \text{A6}$$

$$F - F_{L-pH} = \left(\varepsilon_{L_1} - \varepsilon_{HL_1}\right) \cdot [L_1] \quad \text{A7}$$

At acidic pH range, the $K_{a1}$ can be quantitatively described (Equation A8):

$$\frac{F_{H-pH}-F}{F-F_{L-pH}} = \frac{[HL_1]}{[L_1]} = \frac{[H]}{K_{a1}} \quad \text{A8}$$

Thus,

$$log\,\frac{F_{H-pH}-F}{F-F_{L-pH}} = -logK_{a1} - pH = pK_{a1} - pH \quad \text{A9}$$

The p$K_{a1}$ values were calculated by MATLAB software.

## Appendix B

Dissociation constants (p$K_{a2}$) of PARAFAC components were estimated from decreasing maximum fluorescence intensity ($F$) with the increase of pH at basic condition. At basic pH range, the reactions between PARAFAC component ($L_2$) and hydroxyl ($OH$) can be quantitatively described with 1:1 stoichiometric model (Equations B1 and B2).

$$HL_2 + OH \leftrightarrow L_2 + H_2O \quad \text{B1}$$

The conditional stability constant, $K_t$, and dissociation constant, $K_{a2}$, can be expressed:

$$K_t = \frac{[L_2]}{[HL_2][\mathrm{OH}]} = \frac{K_{a2}}{K_{ow}} \quad \text{B2}$$

During the fluorescence titration, the $F$ is associated to the concentration ($C$) of PARAFAC component ($L_2$) by using the molar fluorescence coefficient ($\varepsilon$) (Equations B3-B5).

$$F_{H-pH} = \varepsilon_{L_2} \cdot C_{L_2} \quad \text{at high pH} \quad \text{B3}$$

$$F_{L-pH} = \varepsilon_{HL_2} \cdot C_{L_2} \quad \text{at low pH} \quad \text{B4}$$

$$F = \varepsilon_{L_2} \cdot [L_2] + \varepsilon_{HL_2} \cdot [HL_2] \quad \text{at middle pH} \quad \text{B5}$$

$F_{\text{H-pH}}$ is for $L_2$, dissociated at high pH; $F_{L-pH}$ is for $HL_2$, dissociated at low pH.

From mass balance of $C_{L_2} = [L_2] + [HL_2]$,

$$F - F_{H-pH} = \left(\varepsilon_{HL_2} - \varepsilon_{L_2}\right) \cdot [HL_2] \quad \text{B6}$$

$$F_{L-pH} - F = \left(\varepsilon_{HL_2} - \varepsilon_{L_2}\right) \cdot [L_2] \quad \text{B7}$$

At basic pH range, the $K_{a2}$ can be quantitatively described (Equation B8).

$$\frac{F-F_{H-pH}}{F_{L-pH}-F} = \frac{[HL_2]}{[L_2]} = \frac{K_{ow}}{K_{a2}\cdot[OH]} = \frac{[H]}{K_{a2}} \quad \text{B8}$$

Thus,

$$log\,\frac{F-F_{H-pH}}{F_{L-pH}-F} = -logK_{a2} - pH = pK_{a2} - pH \quad \text{B9}$$

The p$K_{a2}$ values were calculated by MATLAB software.